Available online at www.sciencedirect.com
ScienceDirect
Nuclear Instruments and Methods in Physics Research A 591 (2008) 147–150
NUCLEAR INSTRUMENTS & METHODS IN PHYSICS RESEARCH Section A
www.elsevier.com/locate/nima

Pulse height fluctuations of integrated micromegas detectors

M. Chefdeville[a,*], H. van der Graaf[a], F. Hartjes[a], J. Timmermans[a], J. Visschers[a], V.M. Blanco Carballo[b], C. Salm[b], J. Schmitz[b], S. Smits[b], P. Colas[c], I. Giomataris[c]

[a]NIKHEF, Kruislaan 409, Amsterdam 1098 SJ, The Netherlands
[b]University of Twente/Mesa+ Institute, Hogekamp 3214, P.O. Box 217, Enschede 7500 AE, The Netherlands
[c]DAPNIA/SPP, Bat. 141, CEA Saclay 91191 Gif sur Yvette cedex, France

Available online 21 March 2008

Abstract

Recent publications report that Micromegas-based detectors exhibit very good energy resolution for gaseous radiation detectors. When made in microtechnology, the physical dimensions of such a detector can be controlled with micrometer precision over a large area. In this paper we report an energy resolution of 5.2% r.m.s. at 5.9 keV of such a detector (called InGrid) and present experimental and simulation results to explain and quantify the contributions to the gain fluctuations. Our results may be applicable also for other micropattern gas detectors.

Keywords: Integrated Micromegas detectors; Gain fluctuations; Fano factor

1. Introduction

Pulse height fluctuations partly determine gaseous detector precision in measuring energy losses and tracks of charged particles and arise mainly from the statistical processes of primary ionization and gas amplification. This also applies to the energy measurement of particles absorbed in the gas, although the primary fluctuations are reduced. In that case the energy resolution R can be expressed as [1]

$$R = \sqrt{W/E \cdot (F + b)} \tag{1}$$

with F the Fano factor, W the mean energy per ion pair, E the particle energy and b the single electron gain distribution relative variance. Although values of W and F are known in various gases [2,3] and gain fluctuations have been extensively studied in wire counters [4], very few measurements of b in Micromegas detectors were published [5].

In this work we report on very good energy resolution of integrated Micromegas detectors (called InGrids) and use Eq. (1) to estimate the contribution from gain fluctuations [6]. This implies to take into account other sources of pulse height variations. For instance it may occur that not all primary electrons cause an avalanche, due to a limited collection efficiency. The gain may vary systematically for electrons following different trajectories in the detector: in particular, the entrance position in the grid hole may be important for the final gas amplification of the electron. Finally, dimensional variations in the detector due to manufacturing imperfections may lead to gain variation across the detector. Measurements and modelling of these effects are presented in Section 3.

2. Experimental setup

InGrid is a Micromegas grid integrated on a silicon wafer by means of planar microfabrication techniques. More details on the detector manufacturing can be found in Ref. [7]. The basic operation of the InGrid detector is reported in Ref. [8].

The InGrid we report on is a 1 μm thin Al grid suspended 59 μm above the wafer by means of SU8 insulating pillars. The grid holes have a diameter of 15.5 μm, a pitch of 32 μm and are made according to a square pattern. The pillars are 30 μm diameter and arranged in a square pattern with a pitch of 128 μm. In that configuration, the pillars are placed

*Corresponding author.
E-mail address: chefdevi@nikhef.nl (M. Chefdeville).

0168-9002/$ - see front matter
doi:10.1016/j.nima.2008.03.045

below some of the grid holes resulting in 6.25% of dead area.

The measurements were performed in a gas mixture of $Ar:CH_4$ 90:10 using an ^{55}Fe source that emits 5.9 keV (Mn K_α) and 6.5 keV (Mn K_β) photons. In order to measure the true resolution at 5.9 keV, the K_β line was almost fully absorbed in a 10 μm thin Cr foil (K-edge at 6.0 keV) placed over the detector kapton window.

Signals were read out from the grid and directed to a low noise charge sensitive pre-amplifier (800 electrons ENC, 1 μs integration time). Further amplification was performed by means of an Ortec amplifier (gain of 6) [9] those output was connected to a PC controlled Amptek portable multi channel analyzer [10] for spectra display and analysis.

3. Measurements

3.1. Collection efficiency

The collection efficiency of Micromegas detectors depends on what fraction of the field lines from the cathode reach the anode and on how well electrons follow these field lines. At the entrance of the amplification region, field lines are compressed by a factor equal to the ratio of the amplification field to the drift field. Above a certain field ratio, almost all the field lines from the cathode end on the anode and any electron from the drift region should enter the amplification region.

At a grid voltage of −390 V, the electric field in the amplification region was 66 kV/cm and the gain was measured to be 2.5×10^3. The ^{55}Fe photo-peak position was measured from drift fields of 30 V/cm up to 1 kV/cm. The peak position P can be expressed as

$$P(E_{\rm drift}) = SN\eta(E_{\rm drift})G(E_{\rm drift}) \quad (2)$$

where N is the mean number of primary electrons, η the collection efficiency, G the detector gain and S a constant term determined by the electronics.

A dependence of the gain on the drift field is observed when the field does not increase steeply from the drift to the amplification region. In that case a reduction of the drift field can reduce the amplification field at the entrance of the hole resulting in longer mean free paths for the first ionization collisions, i.e., lower gains [8].

This effect was quantified by calculating the gain of electrons drifting along the hole axis from cathode to anode. Within the GARFIELD program [11], the grid was modelled by an array of infinitely long 1 μm diameter 1 μm separated parallel wires, providing a reasonably good approximation of the 2D electric field.

The gain was calculated by integrating the Townsend coefficient along the electron path. This procedure was repeated for drift fields of 30 V/cm up to 1 kV/cm. The gain relative variations $\Delta G/G$, evaluated as $G_{1\,{\rm kV/cm}} - (G_{100} - G_{30})/G_{30}$ V/cm for five different grid geometries, are tabulated below (see Table 1).

As expected, the gain dependence on the drift field depends on the grid geometry. The field variation from the drift region to the amplification region is steeper for small hole diameters resulting in less gain sensitivity to drift field variations. Concerning the InGrid geometry we report on (15.5 μm hole diameter) the gain change from 30 to 1000 V/cm equals to 1.3%. Consequently the peak position is a direct indication of collection efficiency. The measured collection efficiency dependence on the field ratio is shown in Fig. 1. It can be seen that the collection reaches a plateau for field ratios larger than 400.

3.2. Electron trajectories

To study the gain dependence on the electron trajectories, a 3D map of the electric field was calculated by the Finite Element Method program MAXWELL3D [12] and loaded into GARFIELD to simulate electron avalanches. Releasing single electrons on several locations across the hole area, the average gain was calculated as a function of the electron entrance position inside the hole.

The integrated electric field experienced by the electron is lowest if it enters the amplification region through the hole center while it increases slightly if the electron passes closer to the grid hole edges, yielding gain variations of 5% r.m.s. over the total hole plane area. This figure is an upper limit

Table 1
Gain increase when raising the drift field from 30 V/cm to 1 kV/cm for a 32 μm hole pitch, 59 μm gap thickness InGrid.

Diameter d (μm)	$\Delta G/G$ (%)
11.5	0.95
13.5	1.03
15.5	1.31
17.5	1.43
19.5	1.57

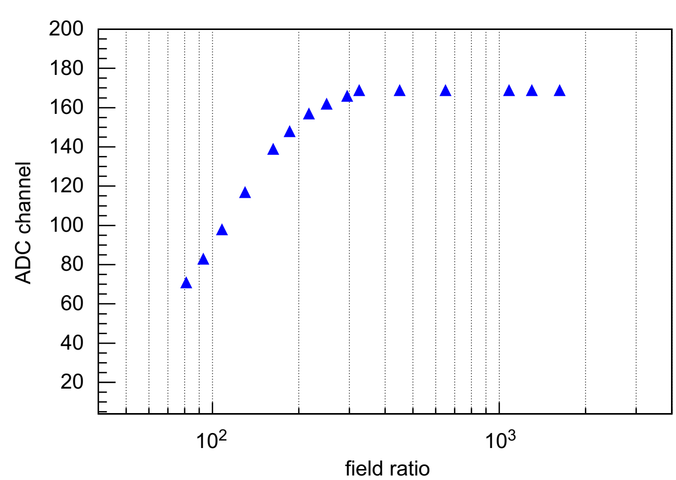

Fig. 1. Measured ^{55}Fe peak position (proportional to collection efficiency in our experiments, see Section 3.1) as a function of field ratio in P10 gas mixture at $E_A = 66$ kV/cm.

as at high field ratio the electron entrance distribution in the hole should be narrow, resulting in smaller fluctuations.

3.3. Geometry inhomogeneities

Measurements of hole diameter and gap thickness yielded, respectively, (15.5 ± 0.5) and $(59 \pm 1)\,\mu$m. The gain sensitivity to diameter variations was studied as described in Section 3.1 and was found to obey the following parametrization:

$$\Delta G/G = -\delta \Delta d \quad (3)$$

with d the hole diameter and δ a parameter that decreases with the gap thickness. At 59 μm gap thickness, δ equals $2.8 \times 10^{-2}\,\mu\mathrm{m}^{-1}$ resulting in gain variations of 1.4%.

A well-known feature of Micromegas detectors is the small gain sensitivity to amplification gap variations: the gain trend with respect to the gap at constant grid voltage presents a maximum. The gap for which the gain is the largest depends mainly on the gas composition [13]. By means of different InGrid prototypes, the gain dependence on the gap could be measured and parametrized by a parabola (Fig. 2).

In consequence, the optimum gap thickness equals 54 μm which is slightly less than the detector gap and the gain fluctuations from the gap variations amount to 7.9%. Gain measurements at 45 and 69 μm gaps were performed, respectively, with 18.9 and 23.0 μm hole diameter InGrids. As we are interested here in gap variations at constant hole diameter (15.5 μm), they were corrected according to Eq. (3).

Adding quadratically contributions from diameter and gap variations, one finds gain fluctuations of 8.1% from geometry inhomogeneities.

3.4. Energy resolution

The detector was operated on the collection plateau ($E_{\mathrm{drift}} = 165\,\mathrm{V/cm}$, field ratio of 400). Two ^{55}Fe spectra were recorded with and without the Cr foil, each

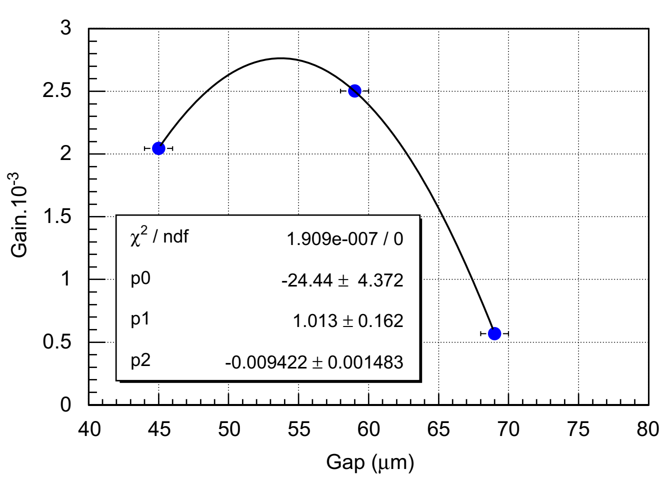

Fig. 2. Gain and gap in P10 gas mixture at −390 V grid voltage. Gains at 45 μm and 69 μm were corrected for hole diameter variations.

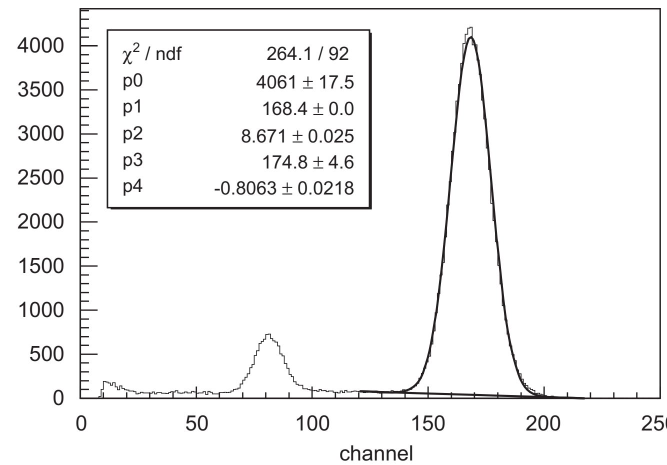

Fig. 3. ^{55}Fe spectrum showing 5.2% r.m.s. on the photo-peak. The 6.5 keV line was strongly attenuated by a Cr foil.

measurement lasting 3 min. The raw spectrum shows a resolution of 5.8% r.m.s. while the filtered one exhibits 5.2% (Fig. 3).

3.5. Gain fluctuations

Correcting the measured energy resolution for the effects described above, 67% single electron gain fluctuations could be calculated using Eq. (1) with W and F values of 27.0 eV and 0.14, respectively [14]. This figure includes the contribution from different electron trajectories which is not accurately known (Section 3.2).

3.6. Summary

Among primary statistics, pulse height fluctuations in InGrid detectors are caused by gain fluctuations (67% r.m.s. per electron in our experimental conditions), gain nonuniformities due to pillar thickness variations (7.9%) and hole diameter variations (1.4%). We can thus conclude that the detector's energy resolution is truly limited by the fundamental stochastic processes in the gas.

4. Conclusion

In this contribution we reported on the energy resolution of integrated Micromegas detectors. A resolution of 5.2% r.m.s. at 5.9 keV was measured in P10 gas mixture, suggesting that only primary and avalanche fluctuations are contributing to signal fluctuations. This statement motivated the study of the various sources of signal fluctuations in InGrid detectors.

It was shown that the techniques used for the detector fabrication permitted an accurate control of hole diameters and amplification gap thicknesses, resulting in only a small contribution of gain inhomogeneities (8.1% r.m.s. per electron). The variance of the single electron distribution in P10 gas mixture at gain of 2.5×10^3 was estimated to be 67% r.m.s., assuming values of W and F from the literature.

References

[1] D. Srdoc, et al., J. Phys B 20 (1987) 4473.
[2] I.K. Bronic, J. Phys B 20 (1987) 4473.
[3] I.K. Bronic, J. Phys B 25 (1992) 215.
[4] G.D. Alkhazov, Nucl. Instr. and Meth. A 89 (1970) 155.
[5] Y. Giomataris, et al., Nucl. Instr. and Meth. A 449 (2000) 314.
[6] D.C. Arogancia, et al., arXiv:0705.2210v1 [hep-ex] 15 may 2007.
[7] M. Chefdeville, et al., Nucl. Instr. and Meth. A 556 (2006) 490.
[8] V.M. Blanco Carballo, et al., Nucl. Instr. and Meth. A 576 (2007) 1.
[9] Ortec, 474 Timing filter amplifier.
[10] Amptek, Pocket MCA 8000A.
[11] R. Veenhof, Nucl. Instr. and Meth. A 419 (1998) 729.
[12] Ansoft, Maxwell Parameter extractor 3D.
[13] Y. Giomataris, Nucl. Instr. and Meth. A 419 (1998) 239.
[14] I.K. Bronic, Nucl. Instr. and Meth. B 71 (1992) 366.